Development 134, 1605-1615 (2007) doi:10.1242/dev.02827

Zebrafish *curly up* encodes a *Pkd2* ortholog that restricts left-side-specific expression of *southpaw*

Jodi Schottenfeld, Jessica Sullivan-Brown and Rebecca D. Burdine*

The zebrafish mutation *curly up* (*cup*) affects the zebrafish ortholog of polycystic kidney disease 2, a gene that encodes the Ca^{2+}-activated non-specific cation channel, Polycystin 2. We have characterized two alleles of *cup*, both of which display defects in organ positioning that resemble human heterotaxia, as well as abnormalities in asymmetric gene expression in the lateral plate mesoderm (LPM) and dorsal diencephalon of the brain. Interestingly, mouse and zebrafish *pkd2*$^{-/-}$ mutants have disparate effects on *nodal* expression. In the majority of *cup* embryos, the zebrafish *nodal* gene *southpaw* (*spaw*) is activated bilaterally in LPM, as opposed to the complete absence of *Nodal* reported in the LPM of the *Pkd2*-null mouse. The mouse data indicate that *Pkd2* is responsible for an asymmetric calcium transient that is upstream of *Nodal* activation. In zebrafish, it appears that *pkd2* is not responsible for the activation of *spaw* transcription, but is required for a mechanism to restrict *spaw* expression to the left half of the embryo. *pkd2* also appears to play a role in the propagation of Nodal signals in the LPM. Based on morpholino studies, we propose an additional role for maternal *pkd2* in general mesendoderm patterning.

KEY WORDS: Zebrafish, *pkd2*, Asymmetry, Left-right axis, Kidney, Pronephros, Laterality, Cilia

INTRODUCTION

The vertebrate body plan is organized into three primary body axes: anterior-posterior (AP), dorsal-ventral (DV), and left-right (LR). Although patterning along the AP and DV axes is readily observable, the internal asymmetries of the left-right axis are masked by an external bilateral symmetry. Instead, it is the asymmetric placement of internal organs that distinguishes the left and right sides. Human laterality disorders arise from defects in left-right patterning and exist in two primary forms: situs inversus and heterotaxia. Situs inversus, characterized by a complete reversal of the viscera, occurs at a rate of about 1 in 20,000 people and is associated with an increased incidence of congenital heart disease (CHD) (Mercola and Levin, 2001; Ramsdell, 2005). Heterotaxia, where one or more organs are positioned incorrectly, can have catastrophic effects on the development of the organism. Approximately 1 in every 8,000 births will result in heterotaxia, which also often manifests as CHD (Mercola and Levin, 2001).

The information necessary for the proper positioning of the viscera is provided by earlier asymmetric events including the left-side-specific expression of Nodal-related signaling factors. In the mouse embryo, asymmetric activation of *Nodal* transcription occurs at the ventral node during gastrulation. The node is lined by an epithelium that has one primary cilium protruding from the surface of each cell. Although cilia located at the node have 9+0 axonemes and are generally thought to be immotile, the presence of *Left-right dynein* (*Ird*; *Dnahc11* – Mouse Genome Informatics) is thought to enable the central population of cilia to rotate in a clockwise direction. This ciliary rotation drives a leftward fluid flow over the node that is necessary for the proper establishment of sidedness, as mutations that compromise ciliogenesis or inhibit the mobility of these cilia result in randomization of the viscera (McGrath and Brueckner, 2003). In teleosts, Kupffer's vesicle is thought to be analogous to the mouse node in the establishment of left-right patterning (Amack and Yost, 2004). A conserved role for ciliary flow in the establishment of left-right asymmetry is supported by motile cilia and flow found at Kupffer's vesicle in zebrafish and *Medaka* embryos (Essner et al., 2005; Kramer-Zucker et al., 2005; Okada et al., 2005). Ciliary flow in the mouse has also been shown to be upstream of an asymmetric calcium flux in the epithelial cells adjacent to the left side of the node (McGrath and Brueckner, 2003), an event that appears to be conserved in chick and zebrafish (Raya et al., 2004; Sarmah et al., 2005). This left-specific intracellular calcium release is thought to be elicited by the flow-induced stretch activation of the calcium channel, polycystic kidney disease 2 (Pkd2), which localizes to the cilia of the mouse node (McGrath et al., 2003).

Human *PKD2* encodes a six-pass transmembrane, Ca^{2+}-activated, non-specific cation channel, termed polycystin 2 (PC2) (Gonzalez-Perrett et al., 2001; Hanaoka et al., 2000; Vassilev et al., 2001). Heterozygous *PKD2* mutations are found in approximately 15% of human autosomal dominant polycystic kidney disease patients (Wu et al., 1997). Mouse embryos homozygous for an inactivated allele of *Pkd2* exhibit severe cardiac and kidney malformations and are embryonic lethal between E13.5 and parturition (Wu et al., 2000). *Pkd2*$^{-/-}$ mice also display laterality disturbances in *Nodal*-related signaling genes, embryonic turning, visceral organs and heart morphogenesis. Most critically, without PC2 activity, no left-specific calcium expression is detected at the node and asymmetric activation of *Nodal* transcription does not occur, resulting in right isomerism (McGrath et al., 2003; Pennekamp et al., 2002). Therefore, current models for the initiation of a left-right symmetry breaking event include a role for PC2 upstream of asymmetric *Nodal* gene transcription. The link connecting this calcium transient with *Nodal* activation in the mouse is still unclear, although evidence exists for the involvement of the Notch pathway (Raya et al., 2004). In this paper, we present evidence for an alternative role of *pkd2* in the development of the left-right axis.

Here we describe our analysis of *curly up* (*cup*), which encodes the zebrafish ortholog of polycystic kidney disease 2. We characterized two alleles of *cup*, and even though one allele of *cup* appears to be a null, *cup* mutants do not display defects in kidney

Department of Molecular Biology, Princeton University, Princeton, NJ 08550, USA.

*Author for correspondence (e-mail: rburdine@princeton.edu)

Accepted 1 February 2007

patterning nor do they develop kidney cysts. *cup* alleles display left-right defects in organ positioning that resemble human heterotaxia, as well as abnormalities in asymmetric gene expression in the lateral plate mesoderm (LPM) and dorsal diencephalon of the brain. Surprisingly, *nodal* expression patterns in the LPM are different in the mouse and zebrafish *pkd2*$^{-/-}$ mutants. In the majority of *cup* embryos, *spaw* is activated bilaterally in LPM. Although defects in the development of the notochord can result in bilateral transcription of *nodal*, we find that the midline structures in *cup* embryos are not compromised. Thus, in zebrafish, PC2 is not responsible for the activation of *spaw* transcription but is required for a mechanism to bias *spaw* expression towards the left half of the embryo.

MATERIALS AND METHODS

Zebrafish strains

cup^{tc321} and *cup*^{ty30b} were obtained from a large-scale ENU mutagenesis screen (Brand et al., 1996; Haffter et al., 1996). Both *cup* mutations were generated in the TU strain and maintained by outcrossing to AB, WIK and PWT. PWT is a wild-type strain generated in our laboratory that has a very low background of left-right defects. The *cup* phenotypes and differences in severity between *cup*^{tc321} and *cup*^{ty30b} have been observed in multiple generations.

Positional cloning of *curly up*

Mapping of the *cup* locus was performed with SSLP markers as described (Liao and Zon, 1999). The *cup* genomic interval was narrowed between markers z10888 and z25625 on chromosome 1. Sequence surrounding these SSLP markers was identified through the Ensembl Sanger Sequence Database. Additional genomic sequence from the region was identified using BAC ends and BAC mate pair analysis to identify overlapping clones and assemble a genetic contig surrounding the *cup* locus. New SSLP markers used to narrow the *cup* genetic interval were created based on the identified genomic sequence: z9697.9 and z11984.6 (z9697.9F, 5′-GGTCCGCT-TTTGGTGCAGAC-3′; z9697.9R, 5′-CTCTCAGCTCCACAAGTCGC-3′; z11984.6F, 5′-CGCTCTCCAGAGAAAACCAC-3′; z11984.6R, 5′-GT-CTGATCGCAGCGGCGG-3′). The following SNP primers were used to confirm linkage with *pkd2*: pkd2LSNPf, 5′-GATGTGCTTGGACGGATC-CTG-3′; pkd2LSNPr, 5′-CACACCTAAAGACACTGTCC-3′.

Sequencing of *cup*^{tc321} and *cup*^{ty30b} and cloning and RT-PCR of *pkd2*

The zebrafish *pkd2* gene was amplified from a 24-hour cDNA library created with the Marathon cDNA Amplification Kit (BD Biosciences) using cup5Bgl2f (5′-CAGATCAGATCTATGAGCTCCAGTCGCGTTCG-3′) and cup3PmeIr (5′-TCTGACGTTTAAACTCACAAGTGGGCGGGGC-3′). The PCR product was cut with *Bgl*II and *Pme*I, and inserted into the *Bgl*II and *Eco*RV sites of vector T7TS (Cleaver et al., 1996). For production of an in situ hybridization probe, a *Bgl*II-*Apa*I fragment from the T7TS-pkd2 plasmid was cloned into pBluescript II SK (+) using the *Bam*HI and *Apa*I sites. Full-length sequence was obtained by 5′ and 3′ RACE. Mutations in *cup*^{tc321} and *cup*^{ty30b} were identified by sequencing genomic DNA.

RT-PCR of the *pkd2* transcript was performed with total RNA isolated from 1-cell, 256-cell, 1K-cell, sphere, and 18-somite stage embryos. cDNA libraries were made with the SuperScript First-Strand Synthesis System for RT-PCR (Invitrogen) and primers located in exon 3 and exon 7 (pkd2 1F, 5′-GTGGAGAGCCAACCAACTTC-3′; pkd2 2R, 5′-CTGAAGCCGA-GCCAGCGGCT-3′) were used to amplify a 700 bp fragment of *pkd2*.

RNA probes and whole-mount in situ hybridization

DIG-labelled RNA probes were transcribed from linearized DNA templates and used in RNA in situ hybridization by standard methods. Antisense probes included *cardiac myosin light chain* (*cmlc2*; *myl7* – ZFIN) (Yelon et al., 1999), *forkhead 2* (*fkd2*; *foxa3* – ZFIN) (Odenthal and Nusslein-Volhard, 1998), *preproinsulin* (*ins*) (Milewski et al., 1998), *southpaw* (*spaw*) (Ahmad et al., 2004), *paired-like homeodomain transcription factor* (*pitx2*) (Yan et al., 1999), *polycstic kidney disease 2* (*pkd2*), *sonic hedgehog* (*shh*) (Krauss et al., 1993; Thisse and Thisse, 1999), *lefty1* (Bisgrove et al., 1999), *lefty2* (Bisgrove et al., 1999), *SRY-box containing gene 17* (*sox17*) (Alexander and Stainier, 1999), *alpha-tropomyosin* (Ohara et al., 1989), *orthodenticle homolog* 5 (*otx5*) (Gamse et al., 2002), *leftover* (*lov*; *kctd12.1* – ZFIN) (Gamse et al., 2003), and *charon* (*char*) (Hashimoto et al., 2004).

Immunofluorescence

Embryos were fixed in Dent's fixative at 4°C overnight, gradually rehydrated into PBDT (1×PBS, 0.1% Tween 20, 1% DMSO), and blocked for 2 hours in PBDT containing 10% normal goat serum (NGS). To visualize cilia, embryos were incubated overnight at 4°C in a 1:400 dilution of monoclonal acetylated tubulin primary antibody (Sigma #T6793) in PBDT. Six 30-minute washes in PBDT containing 1% NGS and 0.1 M NaCl were administered before the last 30-minute wash in PBDT containing 1% NGS. The embryos were incubated overnight at 4°C with FITC-IgG2b at 1:500 (Southern Biotech #1090-02). The following day, the embryos were soaked in Hoechst (Molecular Probes #H3570) for 15 minutes at 1:1250 in PBDT before six additional 30-minute washes with PBDT containing 1% NGS and 0.1 M NaCl. After washing, the embryos were rinsed and stored in Slow Fade buffers (Molecular Probes #S-7461).

Microscopy

Images of live embryos were taken using the ProgressC14 digital camera (Jenoptik) mounted on a Leica MZFL III microscope. Embryos processed for immunofluorescence were mounted in Aqua-PolyMount (Polysciences #18606) and visualized on a Zeiss LSM 510. Embryos processed for in situ hybridization analysis were mounted in modified GMM (Struhl, 1981) [100 ml Canada Balsam (Sigma #C-1795), 10 ml methylsalicylate (Sigma #M0387-100G)], visualized using a Leica DMRA microscope at 10× magnification, and photographed with the ProgressC14 digital camera.

Morpholino injection

Morpholino antisense oligonucleotides (MO) (Gene Tools, LLC) were maintained in 50 μg/μl stock solutions in water at –80°C. The *cup* augMO, 5′-AGCTCATCGTGTATTTCTACAGTAA-3′, spans a portion of the 5′UTR directly upstream of the AUG start site and the start site itself. The *pkd2* augMO [previously reported as *hi4166* MO by Sun et al. (Sun et al., 2004)], 5′-AGGACGAACGCGACTGGAGCTCATC-3′, begins at the start AUG and extends into the first exon. Although these two MOs overlap by 8 nucleotides, only the *pkd2* augMO effectively phenocopied *cup* (1-4 ng). The 9697-S1 splice-site MO, 5′-GAAACGGGCCTTCTGTGAACTACAG-3′, is complimentary to the intron 3-exon 4 splice junction. The 9697-S2 splice-site MO, 5′-TTAACATACGCAGTGCCATTCTTGG-3′, overlaps the exon 4-intron 4 splice junction of the *pkd2* transcript. Only 9697-S1, used at 9 ng per embryo, was successful in phenocopying *cup*. Although this MO is predicted to block splicing, no alterations in the *pkd2* message were observed by RT-PCR. Thus, we believe the 9697-S1 MO is more likely to be blocking translation. In support of this, other splice-site MOs have been shown to block translation of the message (M. Mullins, personal communication), but formal proof will require the generation of antibodies that recognize the Cup protein.

MOs were mixed with 5 mg/ml Phenol Red and injected into 1- to 4-cell stage embryos as described (Gritsman et al., 1999).

Histological analyses

Embryos were fixed in 4% paraformaldehyde (Sigma P6148) in PBS overnight at 4°C, and stored in 4% sucrose in PBS. After a gradual dehydration into ethanol, embedding was performed according to the Electron Microscopy Sciences protocol for JB-4 histology (EMS #14270-00). The embryos were sectioned on a Leica RM2255 Rotary Microtome at 4 μm. Hematoxylin and Eosin staining (all components were in non-alcohol-based solutions) was performed according to laboratory protocols (J.S.-B., unpublished; available upon request).

RESULTS

Mutations in the gene *curly up* affect *pkd2*

To gain insight into the genetic events involved in establishing the left-right axis, we have analyzed *curly up*, a mutation with left-right patterning defects that was originally isolated from a large-scale zebrafish mutagenesis screen as having a tail curl phenotype (Haffter

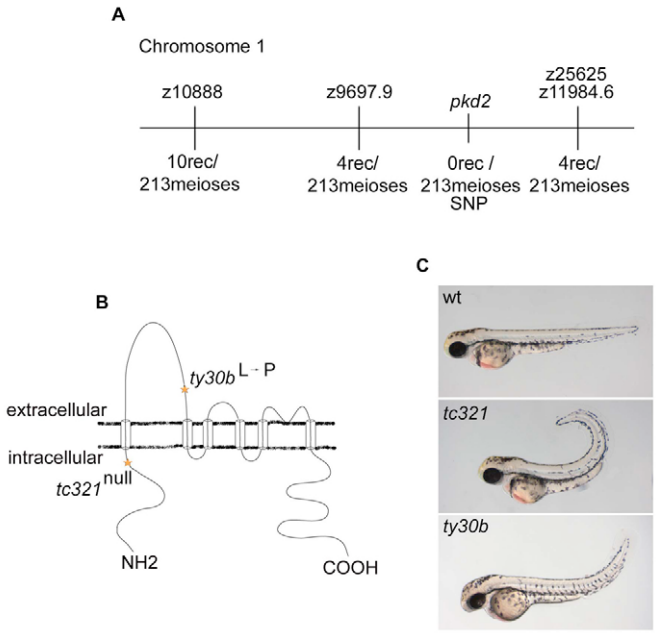

Fig. 1. Identification and structural analysis of *cup/pkd2*. (**A**) Mapping of the *cup* mutation to a genetic interval on chromosome 1. The number of recombinants at each marker is shown. (**B**) *pkd2* encodes a six-pass transmembrane calcium-activated non-specific cation channel [structure modified from Hayashi et al. (Hayashi et al., 1997)]. Sequencing of *pkd2* in *tc321* mutants revealed a nonsense mutation at nucleotide position 407 and *ty30b* showed a missense mutation at nucleotide position 1052, resulting in an amino acid substitution from a leucine to proline. (**C**) Lateral image of wild-type, cup^{tc321}, and cup^{ty30b} embryos at 48 hpf. Both alleles have a curly tail upward phenotype, but *ty30b* has a milder curvature than that of *tc321*.

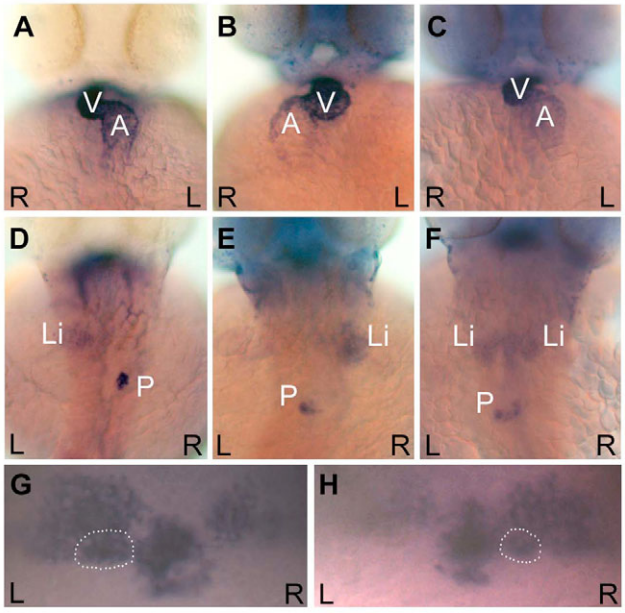

Fig. 2. *curly up* embryos display defects in visceral and brain asymmetries. Ventral views of the heart (**A-C**) and dorsal views of the liver and pancreas (**D-F**) in *cup* embryos at 48 hpf. The heart, liver and pancreas were visualized by in situ hybridizations for *cmlc2*, *fkd2*, and *ins*, respectively. Wild-type organ positioning can be seen in approximately one third of a *cup* mutant population (A and D), where the ventricle loops to the right (A), and the liver resides on the left and the pancreas on the right (D). *cup* embryos also exhibit situs inversus, as seen by the complete reversal of the heart (B), liver and pancreas (E). Approximately one-third of *cup* mutants display heterotaxia. Included in this category was an embryo that had correct heart looping (C) but showed a duplicated liver with a reversed pancreas (F). (**G**,**H**) Dorsal views of the habenular nuclei and the pineal complex in 3-day *cup* embryos. The parapineal is outlined in each panel. (G) *cup* mutant with the wild-type pattern of more intense *lov* expression in the left habenula, and left parapineal placement visualized by *otx5*. (H) *cup* mutant with reversed diencephalic asymmetries. L, left; R, right; V, ventricle; A, atrium; Li, liver; P, pancreas.

et al., 1996). We utilized positional cloning techniques to identify the gene affected in the *cup* mutant. The *cup* mutation was placed on chromosome 1 using bulk segregant analysis (Talbot and Schier, 1999). Subsequent analysis was performed on 213 meiotic events to narrow the chromosomal location of *cup* to a 6.6 cM interval between simple sequence-length polymorphism (SSLP) markers z10888 and z25625 (Liao and Zon, 1999). We assembled a set of genomic clones that span the *cup* locus using available genomic sequence from the Sanger sequencing project. New SSLP markers were then created from these contig sequences (z9697.9 and z11984.6) and used to further refine the location of the *cup* mutation to a 2.6 cM region. One likely candidate for *cup* in this region was the gene *pkd2*, based on left-right defects observed in *Pkd2* mutant mice (Pennekamp et al., 2002). Therefore, we used the 3′ untranslated region of the *pkd2* transcript to generate a single nucleotide polymorphism (SNP) marker. SNP mapping of *cup* recombinant embryos revealed no recombination between *pkd2* and the *cup* locus (Fig. 1A).

The zebrafish *pkd2* transcript is 3.5 kb in length and encodes a 904 amino acid protein that is the zebrafish homolog of polycystin 2 (PC2) (Fig. 1B). PC2 is a Ca^{2+}-sensitive cation channel with six hydrophobic stretches and intracellular N- and C-termini (Gonzalez-Perrett et al., 2001; Hanaoka et al., 2000; Vassilev et al., 2001). Zebrafish *pkd2* shares 67% and 65% identity, and 78% and 79% similarity, with the human and mouse orthologs, respectively (over 900 and 899 amino acid alignments; data not shown). Similarities include signaling elements such as an EF-Hand and a coiled-coil domain that are located in the C-terminus of the protein (Delmas et al., 2004).

To verify that *pkd2* is mutated in *cup*, each Ensembl-predicted exon was sequenced from *cup* genomic DNA of two different alleles, cup^{tc321} and cup^{ty30b}. Comparisons between the sequence of wild-type sibling embryos and cup^{tc321} embryos identified a nonsense mutation in exon 2 that is predicted to generate a truncated protein consisting of only the N-terminal 135 residues (Fig. 1B). *ty30b* embryos have a missense mutation in exon 5 that changes a T to a C at nucleotide 1052, substituting a proline for a leucine in the first extracellular loop of the protein (Fig. 1B). We originally defined cup^{tc321} as a stronger allele than cup^{ty30b} based on the severity of the tail curl phenotype (Fig. 1C). Since *tc321* is likely to be a molecular null based on its predicted protein product, the mutations for each allele are consistent with *tc321* being a stronger loss-of-function allele than *ty30b*. The mouse anti-PC2 antibodies p57 and 58 recognize an antigenic region that includes the conserved leucine residue mutated in *ty30b* embryos. These antibodies can block PC2-dependent intracellular calcium release from ER stores (Nauli et al., 2003), and we therefore predict that a mutation in this region of the protein would interfere with proper channel activity.

Table 1. Defects in visceral and brain asymmetries in *cup* mutant embryos

	Viscera				Brain		
Genotype	*n*	Situs solitus (%)	Situs inversus (%)	Heterotaxia (%)	*n*	Correct (%)	Reversed (%)
Wild type	100	97.0	0.0	3.0	74	97	3
cup^{tc321}	97	35.0	33.0	32.0	41	41	59
cup^{ty30b}	98	37.8	45.9	16.3	85	45	55
augMO (2ng)	54	53.7	35.2	11.1	–	–	–
SpMO (9ng)	23	39.1	26.1	34.8	–	–	–

Viscera and brain data were collected at 48 hpf and 72 hpf, respectively. MOs were injected between the one- and four-cell stage. The laterality defects associated with 2 ng of *pkd2* augMO are less severe than those in embryos injected with a higher dosage, but more general patterning defects can be seen at higher MO concentrations.

cup embryos display defects in visceral and brain asymmetries

cup mutants were reported to have defects in cardiac looping and jogging (Chen et al., 1997). To determine the extent of laterality defects in *cup* mutants, we analyzed the position of the heart (*cmlc2*), liver (*fkd2*), and pancreas (*ins*) in *cup* embryos at 48 hours post-fertilization (hpf) using RNA in situ hybridization with markers for these organs. In a wild-type zebrafish embryo, the ventricle of the heart loops towards the right and the atrium loops towards the left, the liver is positioned to the left of the midline and the pancreas lies to right of the midline (Fig. 2A,D). This wild-type pattern was observed in 35% of *tc321* and 38% of *ty30b* embryos, whereas 33% of *tc321* and 46% of *ty30b* mutants showed a complete reversal in the placement of these organs (Fig. 2B,E, Table 1). A heterotaxic phenotype was seen in 32% and 16% of *tc321* and *ty30b* embryos, respectively (Fig. 2C,F, Table 1). Since our mutant population has a clear increase in defects over background, we conclude that *cup* is globally affecting left-right organ placement.

Asymmetric neural patterning is defined by the unilateral positioning of the parapineal organ that lies to the left of the pineal organ in the zebrafish epithalamus starting at day 2 of development. By day 4, a left-right neural asymmetry can also be found in the dorsal habenular nuclei, where the left habenula has more neuronal projections than the right habenula (Concha et al., 2000; Gamse et al., 2002; Gamse et al., 2003). In *cup* mutant embryos, 40-45% display denser projections on the left side as compared with the right, whereas 55-59% show predominant expression of habenula marker genes on the right side. Thus, *cup* mutants exhibit random placement of neural asymmetric structures across the midline, although the parapineal and larger habenula always remain paired (Fig. 2G,H, Table 1).

cup affects asymmetric gene expression in LPM and brain

Expression of the zebrafish *nodal* gene *southpaw* (*spaw*) and downstream targets *pitx2*, *lefty1* and *lefty2* are restricted to the left LPM during late somitogenesis prior to proper asymmetric localization of organs at 48 hpf (Ahmad et al., 2004). To address how early *cup* affects left-right patterning, expression of *southpaw*, *pitx2* and *lefty1/2* was examined in clutches of 20- to 22-somite embryos from two heterozygote parents for the *cup* mutation (Table 2). Although 25% of embryos within the clutch should be homozygous mutant for *cup*, correct expression of *spaw* at Kupffer's vesicle was observed in all embryos analyzed (data not shown). This is consistent with the finding that the mouse *Pkd2* mutation does not affect *Nodal* expression in the mouse node. By contrast, both *cup* alleles showed increased frequency of bilateral, right-sided, or absent *spaw* expression in the LPM, with bilateral expression being the most common (Fig. 3A-D, Table 2). The bilateral *spaw* expression can be further classified into three categories: bilateral expression extending into the anterior cardiac LPM (Fig. 3B, Table 3); bilateral expression restricted to the posterior portion of the LPM (Fig. 7C, Table 3); and uneven expression on both the left and right sides, where *spaw* propagates anteriorly on one side and remains posterior on the other half (Fig. 7B, Table 3). In embryos that expressed *spaw* only posteriorly, *lefty* was never expressed in the cardiac mesoderm or dorsal diencephalon (Fig. 3H, Table 3, Fig. 7C,D). When *spaw* did extend anteriorly, expression of *lefty* correlated with the left-right placement of *spaw* (Fig. 3A-C, Fig. 7A,B,D, Table 3). Equivalent *spaw* expression in the anterior LPM resulted in randomized *lefty* expression in the heartfield. *pitx2* expression was also randomized in the LPM for both alleles (Table 2). Thus, zebrafish *cup* mutants do differ from mouse *Pkd2* mutants, which are reported to exhibit a loss of *Nodal* in the LPM. However, the mouse mutant expresses *Pitx2* bilaterally only in the posterior LPM, similar to the *spaw* phenotype in *cup* mutants.

Defects in the development of the notochord and/or floorplate can result in bilateral transcription of *nodal* leading to left-right patterning abnormalities (reviewed by Roessler and Muenke, 2001). Since *cup* is expressed in the floorplate in zebrafish (see below), we investigated whether notochord or floorplate development is affected in *cup* mutants by examining expression of *shh* and *lefty1* in 12-

Table 2. Alterations in asymmetric gene expression in *cup* mutant embryos

		spaw					*pitx2*					*lefty1/2*				
Tissue	Genotype	*n*	L (%)	B (%)	R (%)	A (%)	*n*	L (%)	B (%)	R (%)	A (%)	*n*	L (%)	B (%)	R (%)	A (%)
LPM	Wild type	90	93.3	5.6	0.0	1.1	116	95.7	3.4	0.9	0.0	27	100	0.0	0.0	0.0
	cup^{tc321}	114	73.7	20.2	6.1	0.0	192	63.6	16.2	16.6	3.6	114	69.3	1.8	3.5	25.4
	cup^{ty30b}	102	57.8	29.5	2.9	9.8	168	64.9	15.5	19.6	0.0	95	57.9	3.1	7.4	31.6
Brain	Wild type	–	–	–	–	–	116	94.8	1.7	0.9	2.6	27	100	0.0	0.0	0.0
	cup^{tc321}	–	–	–	–	–	101	55.4	3.0	4.0	37.6	114	67.6	1.7	1.7	29.0
	cup^{ty30b}	–	–	–	–	–	169	58.0	5.3	9.5	27.2	95	50.5	2.1	4.2	43.2

L, left; B, bilateral; R, right; A, absent.
The mutant data above reflect the defects seen in clutches of embryos from a cross of *tc321* and *ty30b* heterozygote parents. Therefore, the large percentage of left-sided expression of *spaw* and *pitx2* is due to the approximate 75% of the population of embryos that are wild type or heterozygotes. Percentages of left-sided expression that are less than 75% may be attributed to errors in staging.

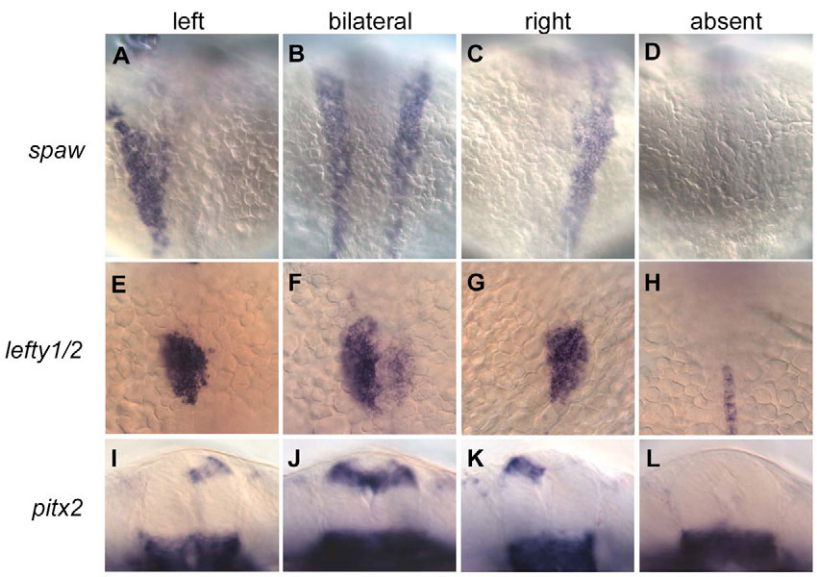

Fig. 3. *curly up* affects expression of left-specific genes in the lateral plate mesoderm (LPM) and dorsal diencephalon. Dorsal views of *spaw* (**A-D**) and *lefty1/2* (**E-H**) expression in 20- to 22-somite stage embryos (A-H) and ventral views of *pitx2* expression in the dorsal diencephalon of 24-somite stage embryos (**I-L**) from *cup* heterozygote crosses. Alterations from normal left asymmetric Nodal signaling in the LPM (A) in *cup* mutants include bilateral (B), right (C), and absent (D) expression of *spaw* in this tissue. Over half of the bilaterally expressing embryos show only posterior propagation of *spaw*. Similarly, asymmetrically expressed downstream targets of Nodal signaling in the LPM and brain are also disrupted. *lefty1/2*, which are normally expressed in the left cardiac LPM (E), have bilateral (F), right (G), and absent (H) expression patterns in *cup* mutants. In H, midline expression of *lefty1* can also be seen. *pitx2*, which is normally expressed on the left side of the diencephalon (I), can be expressed bilaterally (J), on the right (K), or not at all (L) in *cup* embryos. The majority of embryos show no expression of *lefty1/2* in the LPM and diencephalon and no expression of *pitx2* in the diencephalon.

somite and 18-somite embryos, respectively. In wild-type embryos, *shh* is expressed in the notochord and floorplate of the midline and *lefty1* is present only in the notochord. Both gene products showed normal expression patterns in *pkd2*-deficient embryos (data not shown). Expression of *alpha-tropomyosin* was also unaltered in mutant embryos at 8 somites and 24 hpf, indicating that somitogenesis was proceeding normally (data not shown). Since midline structures appeared unaffected in *cup* mutants, the bilateral *spaw* expression cannot be explained by a compromised midline. Thus, in the zebrafish embryo, *pkd2* appears to be responsible for restricting *spaw* transcription to the left side of the LPM. In addition, because we observe a high percentage of *spaw* and *pitx2* expression confined to the posterior LPM, we propose that *pkd2* plays an additional role in the propagation of *nodal* signals in this tissue.

pitx2 and *lefty1* are also transcribed asymmetrically at 24 somites in the dorsal diencephalon of the zebrafish brain (Essner et al., 2000). *cup* embryos exhibited abnormal expression in the brain with the majority of embryos showing a loss of expression of these Nodal target genes (Fig. 3E-H, Table 2). Thus, *pkd2* may play a role in the zebrafish diencephalon in sending or receiving an asymmetric signal from the LPM.

Expression analysis of *pkd2*

To determine where PC2 activity is required for proper left-right patterning, expression patterns of *pkd2* were analyzed by RNA in situ hybridization. Whereas mouse *pkd2* is expressed ubiquitously (Pennekamp et al., 2002), we found distinct expression domains for *pkd2* in zebrafish. Transcription of *pkd2* was first detected at the onset of epiboly in cells marking dorsal fates at dome stage (Fig. 4B). Transcript levels increased as gastrulation continued, with expression expanding into the dorsal marginal cells (Fig. 4D,F). Since transcripts cannot be detected at dome stage and at 40% epiboly in MZ*oep* embryos, which lack most of the mesendoderm, *pkd2* is expressed in mesodermal and endodermal precursor cells during gastrulation (Fig. 4C,E). *pkd2* also localized to the shield and dorsal forerunner cells (DFCs) (Fig. 4F,J). The DFCs maintained expression of *pkd2* as they migrated towards the posterior, leading to a concentrated area of expression at the tailbud (Fig. 4G,K). These transcripts began to become more diffuse as the DFCs formed Kupffer's vesicle. *pkd2* mRNA was present in a ring-like pattern outlining the vesicle during early somite formation, but became less visible as somitogenesis proceeded. A low level of expression could be seen in the neural floorplate and pronephric duct primordia during these later stages (Fig. 4H,I,L).

Although not visible by RNA in situ hybridization, a maternal contribution of *pkd2* mRNA was detected by RT-PCR at 1-4 cells and 256 cells, both of which are stages prior to the mid-blastula transition (1000 cells) (Fig. 4A). Since Kupffer's vesicle has been implicated in left-right patterning in zebrafish, we predict that PC2 might be acting in this structure to affect left-right patterning (Amack and Yost, 2004; Essner et al., 2005). While this manuscript was in preparation, Bisgrove et al. found that injection of morpholinos against *pkd2* to specifically knockdown translation of PC2 in Kupffer's vesicle resulted in left-right patterning defects, supporting a role for PC2 in this location (Bisgrove et al., 2005). *cup* embryos do have a structurally intact Kupffer's vesicle as seen by light microscopy during mid-somitogenesis, and *sox17* expression highlights the proper migration of DFCs towards the tailbud region in mutants during late epiboly stages (data not shown). RNA in situ hybridization for *charon*, a known Nodal inhibitor expressed at Kupffer's vesicle, also shows normal expression patterns in *cup* mutant embryos (data not shown) (Hashimoto et al., 2004). These data indicate that *pkd2* is not responsible for the formation of Kupffer's vesicle, but rather is acting from within the vesicle to affect asymmetric *spaw* expression.

Morpholino knockdown of *pkd2*$^{-/-}$ results in additional cystic phenotypes in a concentration-dependent manner

We created several morpholinos against the *pkd2* transcript. Two MOs were able to effectively phenocopy the *cup* phenotype, one directed against the *pkd2* start site (augMO), and one directed against an intron-exon junction (MO 9697-S1). Alterations in organ positioning and asymmetric *spaw* expression were examined in order to assess the left-right patterning abnormalities in *pkd2* morphants. Although the morphants displayed slightly milder tail curling (Fig. 5A-D), the laterality defects associated with the MO knockdowns were comparable to those of *cup* mutants (Table 4). Interestingly, *pkd2* morphants also exhibited hydrocephalus and dilations in the pronephric region, neither of which was displayed in

Table 3. Expression of *lefty* in cardiac LPM correlates with expression of *spaw* in anterior LPM

		lefty expression in the heartfield			
***spaw* expression**	*n*	Left	Right	Bilateral	None
Anterior and posterior expression					
Left	83	79	–	–	5
Right	4	–	3	–	1
Bilateral (equal)	2	–	–	2	–
Bilateral (left anterior; right posterior)	2	–	–	–	2
Bilateral (right anterior; left posterior)	1	–	1	–	–
None	0	–	–	–	–
Posterior expression only					
Left	0	–	–	–	–
Right	3	–	–	–	3
Bilateral (equal)	18	–	–	–	18

In situ hybridization for *lefty1/2* and *spaw* were performed simultaneously in a clutch of *cup*^{tc321} embryos. Embryos with expression of *spaw* in the area of the heartfield are scored as having anterior expression.

cup mutants (Fig. 5E,L). A number of genes known to cause cystic kidney phenotypes in other model organisms when mutated have been shown to cause pronephric cysts in zebrafish mutants and morphants (Kramer-Zucker et al., 2005; Liu et al., 2002; Otto et al., 2003; Sun and Hopkins, 2001), and MOs to *pkd2* have been reported to cause kidney cysts (Sun et al., 2004). Thus, the finding that the pronephric region is dilated in our *pkd2* morphants is not unexpected. However, we note that the dilations in our morphants are more elongated and are more restricted to the glomerulus than those seen in other pronephric mutants and morphants in the laboratory, and may not be representative of true pronephric cysts (our unpublished data). In fact, in *cup* mutants, severe edema is observed by day 6 in all tissues, suggestive of a general loss in fluid homeostasis not restricted to the pronephros or neural tube.

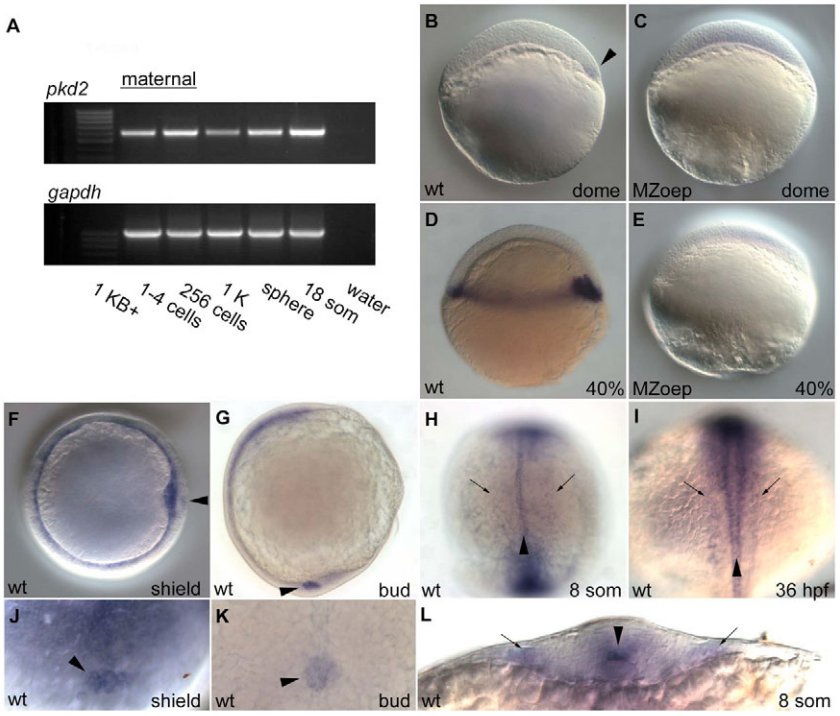

Fig. 4. Expression analysis of *pkd2*. (**A**) RT-PCR of *pkd2* at early developmental time-points shows presence of maternal *pkd2* prior to mid-blastula transition at 1K stage. *gapdh* was used to control for variations in total RNA for each cDNA library. Maternal contribution of *pkd2* RNA cannot be detected by in situ hybridization. (**B-E**) Lateral views of *pkd2* expression patterns in wild-type (B,D) and MZ*oep* (C,E) embryos; anterior is up. Expression of *pkd2* is first noticeable at dome stage, where *pkd2* expression marks the dorsal side of the embryo (arrowhead in B) and continues to be expressed in all dorsal marginal cells by 40% epiboly (D). *pkd2* expression is in mesendodermal tissue as expression is lost in MZ*oep* embryos (C,E). (**F**,**J**) *pkd2* RNA is detected at the shield in gastrulating embryos, as well as in the dorsal forerunner cells (DFCs, arrowhead in F and J; F anterior view, dorsal to the right; J is a higher magnification dorsal view focusing on the DFCs). (**G**,**K**) At tailbud stage, *pkd2* is detected in a circular patch of cells that will soon form Kupffer's vesicle (arrowhead in G and K; G lateral view, anterior is up, dorsal to the left; K is a higher magnification posterior view of region in G denoted by the arrowhead). (**H**,**I**,**L**) Dorsal view of 8-somite (H) and 36-hpf (I) embryos and cross-section view of an 8-somite embryo (L). Faint *pkd2* expression highlighting the pronephric collecting ducts is marked with arrows and the more intensely stained floorplate in the midline is marked with arrowheads.

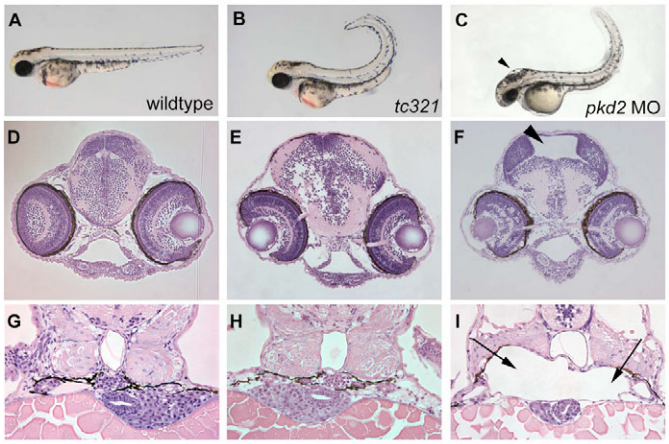

Fig. 5. Morpholino knockdown of *pkd2*$^{-/-}$ causes hydrocephalus and dilations in the pronephric region in high doses. (**A-C**) Lateral views of 48-hpf embryos. Cross-sections of the brain (**D-F**) and kidney regions (**G-I**) at 72 hpf. The *pkd2* augMO (4 ng) (C) and *pkd2* SpMO (not shown) often have variably milder tail curls than that of a *cup*^{tc321} mutant (B) but noticeably different than that of a wild-type embryo (A). The embryos injected with either MO displayed hydrocephalus (F, SpMO) and dilations in the glomerular and tubular regions of the pronephros (I, SpMO) that are not observed in wild-type and *cup* embryos (D,E and G,H). Arrowheads indicate regions of hydrocephalus (C,F) and arrows indicate the dilations in the area of the pronephros (I). Note the smaller liver and gut tube underlying the pronephric dilations in MO-injected embryos (I).

Additionally, *cup* morphants have defects in body size and organ morphology, suggesting that the MOs cause more global organ patterning defects that could be the cause of the pronephric dilations we observe (see below).

Since *cup*^{tc321} is likely to be a molecular null, the additional phenotypes seen in the *pkd2* morphants were somewhat unexpected. To ensure that the N-terminus of PC2 that might be present in *cup*^{tc321} embryos would be unable to account for these phenotypic differences, we supplied 9697-S1 splice morphants with the N-terminal fragment of *pkd2* upon injection at the 1-4 cell stage. The N-terminus of PC2 was unable to rescue any of the additional phenotypes in these morphants (data not shown). Another possibility is that the MOs are removing the maternal contribution of *pkd2*, leading to a more severe phenotype. To determine if the additional phenotypes we observe are indeed due to a more severe loss of *pkd2*, the dependence of these phenotypes on *pkd2* augMO concentration was analyzed. Left-right defects in organ placement and *spaw* expression were evident at the lowest concentration tested (1 ng augMO per embryo), but the curly tail phenotype did not appear until 2 ng of augMO per embryo (Table 4 and data not shown). Dilations in the pronephric area occurred in a low percentage of embryos at this concentration, but increased in frequency with increasing MO concentration (Table 4). Hydrocephalus was only present in a small population of morphants that had been injected with 4 ng of *pkd2* augMO (Table 4). However, at this concentration general body defects were observed, including narrowed axes, smaller heads and overall loss of proper organ development. The pancreas and liver were often positioned on the midline and much smaller than in wild-type embryos (Fig. 5I). The glomerulus of the kidney was also often indiscernible in sectioned embryos (Fig. 5I). Thus, left-right patterning is most sensitive to decreases in *pkd2* levels, followed by the tail curl and dilation phenotypes, respectively. Overall, these results suggest that zygotic *pkd2* is required for left-right patterning and proper tail elongation, whereas loss of maternal *pkd2* results in more severe body defects, perhaps owing to mispatterning in the mesendoderm where *pkd2* is expressed.

cup mutants display no obvious structural ciliary defects

Primary cilia exist on the cells that line the ventral node of the mouse embryo. PC2 localizes to these cilia and has been shown to be responsible for eliciting an asymmetric calcium surge in the epithelial cells adjacent to the left side of the node (McGrath et al., 2003). Cilia also reside on the cells of Kupffer's vesicle in the zebrafish embryo (Essner et al., 2002). To determine if cilia are affected in *cup* morphant and mutant embryos, an antibody against acetylated tubulin was used to visualize cilia by immunofluorescence. As the curly tail phenotype cannot be seen in *cup* mutants until 33 hpf, *pkd2* augMO morphants were analyzed at 12 somites for the presence of cilia on Kupffer's vesicle. The cilia at Kupffer's vesicle in *pkd2* morphants appeared structurally intact (Fig. 6A,B), as did the cilia lining the collecting ducts of the kidney in *cup* mutants at 33 hpf (Fig. 6C,D). Because the formation of Kupffer's vesicle is unaffected in *pkd2* mutants and morphants, it was not surprising to see the same circular distribution of cilia in the morphant embryos. Although no obvious structural abnormalities are detected in the cilia of *pkd2* mutant zebrafish, we cannot rule out the possibility that the cilia might be functionally compromised.

DISCUSSION

The requirement for *pkd2* in left-right patterning is conserved, but the role of *pkd2* might not be

In this study, we identify *pkd2* as the gene affected in the zebrafish *cup* mutant. *pkd2* encodes the cation channel PC2, one of two proteins that are mutated in human polycystic kidney disease (Wu et al., 1997). Similar to the *Pkd2* knockout mouse, *cup* mutants exhibit a variety of

Table 4. Morpholino knockdown of PC2 results in laterality, kidney and mesendoderm defects in a concentration-dependent manner

	Viscera					Pronephric	
[*pkd2* augMO]	*n*	Situs solitus (%)	Situs inversus (%)	Heterotaxia (%)	Abnormal (%)	*n*	Dilation (%)
Control	45	100.0	0.0	0.0	0.0	29	0.0
1 ng	66	63.6	27.3	9.1	0.0	38	5.3
2 ng	54	53.7	35.2	11.1	0.0	44	65.9
3 ng	84	25.0	42.9	6.0	26.1	53	60.4
4 ng	56	0.0	0.0	0.0	100.0	46	97.8

Injections were performed between the one- and four-cell stage in a 5 mg/ml Phenol Red solution. Control injections were with Phenol Red solution alone. The abnormal viscera category includes endoderm defects ranging from multiple liver and pancreata, to thinner body axes that only allowed for midline and improperly shaped abdominal organs. At 4 days, the injected embryos had what appeared to be cystic pronephric regions that differed in size and shape as compared with our normal definition of a kidney cyst. Therefore, we refer to this phenotype as a kidney dilation. Embryos injected with 2 ng or more of the augMO had upward curvatures in their body axes.

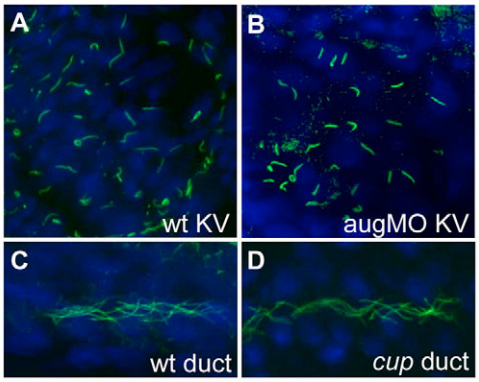

Fig. 6. No obvious structural defects in cilia in Kupffer's vesicle or pronephric ducts of *pkd2* morphant and mutant embryos. (**A-D**) Immunofluorescence performed with antibody against acetylated tubulin that allows for visualization of cilia. Cilia at Kupffer's vesicle in wild-type and *pkd2* augMO embryos at 12 somites (A,B), and cilia in the pronephric ducts in wild type and in cup^{tc321} mutants (C,D), are similar in shape and length. Wild-type Kupffer's vesicle cilia are 4.7±1.4 μm and *pkd2* augMO Kupffer's vesicle cilia are 4.6±1.3 μm in length.

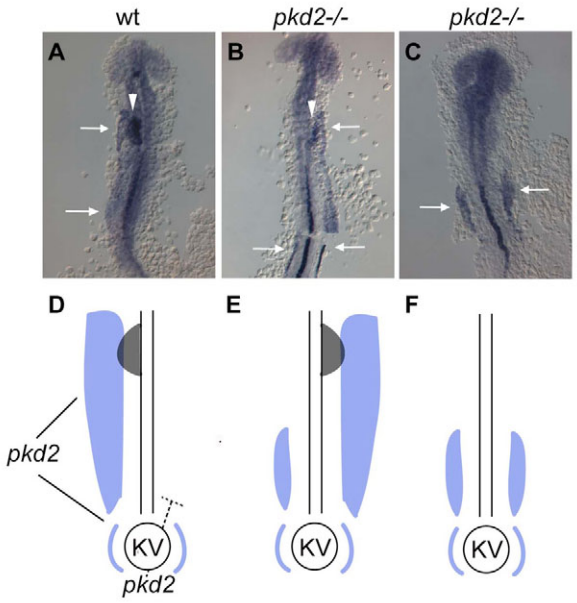

Fig. 7. A model for altered asymmetric *nodal* gene expression in *pkd2*-deficient zebrafish embryos. (**A-C**) RNA in situ hybridization for *spaw* and *lefty1/2* in 20-somite embryos that were flat-mounted in order to see all domains of expression. All panels show *lefty1* staining in the midline. White arrows mark the anterior and posterior areas of *spaw* expression and white arrowheads mark *lefty* expression in the heart field. (**D-F**) Schematic interpretations of A-C (*spaw* in blue, *lefty* in gray). In a wild-type embryo (A,D), *spaw* is expressed in a posterior-to-anterior pattern on the LPM from 10 somites through 22 somites. *lefty1/2* is activated in the left heartfield, the anterior portion of the LPM, beginning at 18 somites. RNA in situ hybridizations for *spaw* and *lefty1/2* together in *cup* mutants (B,C) reveal a role for the anterior domain of *spaw* in the activation of the asymmetric expression of *lefty1/2* in the cardiac LPM. In all embryos scored, *lefty* expression is only apparent in embryos where *spaw* reaches the anterior LPM and it always correlates with the side of *spaw* expression (A,B,D,E). *cup* mutants primarily exhibit bilateral expression of *spaw* to varying degrees of posterior to anterior extension (B,C,E,F). Bilateral anterior expression of *spaw* results in randomized *lefty* expression, where the heartfield will have left, right, bilateral, or absent *lefty*. Bilateral posterior expression of *spaw* always correlates with loss of *lefty* expression in the LPM (C,D). Therefore, because *pkd2* zebrafish mutants display a defect in *spaw* propagation, *lefty*-expressing cells are largely absent from the LPM. In zebrafish, we propose that *pkd2* is acting at Kupffer's vesicle (KV) to restrict *spaw* to the left side of the embryo and that *pkd2* plays an additional role in the proper propagation of *spaw* anteriorly in the LPM (D). *pkd2* could also restrict *nodal* to the left by acting at Kupffer's vesicle to repress *nodal* activation and propagation on the right LPM (D).

organ laterality defects, supporting a conserved requirement for *pkd2* function in left-right patterning. In *pkd2* mutant zebrafish, *spaw* and *pitx2* are both expressed bilaterally in the LPM, and the majority of *spaw* expression is restricted to the posterior. *lefty* expression is absent in the cardiac LPM in the majority of *cup* embryos, although we believe the absence of asymmetric *lefty* is due to the inability of *spaw* to propagate in the LPM in embryos lacking PC2 (Fig. 7). We also find discordance in the percentage of embryos expressing bilateral *spaw* and right-sided *pitx2* in *cup* mutants. We attribute these differences to the following possibilities. Since *spaw* expression is often uneven in its anterior propagation in *cup* mutants, the side that receives the *spaw* signal more prevalently will be the side to express *pitx2*. Alternatively, although *spaw* is thought to act directly upstream of *pitx2*, it is possible that *spaw* is not the sole regulator of *pitx2* in the LPM during these stages.

In mouse, the proposed role for PC2 in activation of Nodal signaling is a prominent feature of the 'two-cilia' model. In this model (reviewed by Tabin and Vogan, 2003), cilia-generated 'nodal-flow' is thought to bend non-motile cilia at the left edge of the node and activate PC2. Flow activation of PC2 leads to an increase in calcium at the left edge of the node, which results in activation of the *Nodal* signaling pathway on the left by an unknown mechanism. Aspects of this model are based in large part on the *Pkd2* knockout mouse, as calcium is not upregulated on the left side of the node and *Nodal* is not activated in the LPM (McGrath et al., 2003; Pennekamp et al., 2002). However, our work convincingly demonstrates that *spaw* is expressed in embryos lacking the PC2 channel and suggests that the role of PC2 is to restrict *spaw* to the left LPM.

The differences between *cup* and the $Pkd2^{-/-}$ mouse with regards to *nodal* expression are significant and call into question the validity of strictly applying current models for PC2 function in left-right patterning to zebrafish. It is clear that some aspects of the two-cilia model are valid in zebrafish, but others are not. For example, Kupffer's vesicle is ciliated and there is a fluid flow in this vesicle, but the flow is reported to be circular, and does not have a left bias (Essner et al., 2005; Kramer-Zucker et al., 2005). A number of calcium asymmetries surrounding Kupffer's vesicle have been reported (Sarmah et al., 2005; Webb and Miller, 2000). However, which calcium asymmetries may be relevant for the establishment of the left-right axis and how calcium asymmetries may function in this process are not clear.

One possible explanation for the differences between mouse and zebrafish is that the role for *pkd2* in left-right patterning is conserved, but the actual function the channel plays in each organism is not. This would be similar to the situation for Fgf8, which has a conserved role in left-right patterning, but is reported to act as a left-determining factor in mouse and a right-determining factor in chick and rabbit (Boettger et al., 1999; Fischer et al., 2002; Meyers and Martin, 1999). It should be noted, however, that two out of 12 *Pkd2* mutant mice described by Pennekamp et al. exhibited bilateral expression of *Nodal*

in the LPM (Pennekamp et al., 2002). Intriguingly, a large percentage of the mouse mutants do exhibit bilateral *Pitx2* expression, a downstream target of *Nodal* signaling, and the domain of expression is restricted to the posterior portion of the embryo (Pennekamp et al., 2002), similar to the posterior expression of *spaw* in *cup* mutants. Thus, it is fair to conclude that *Nodal* signaling can be initiated in the mouse in the absence of PC2, and that the bias of left-sided expression is now lost. This is similar to our findings in fish and suggests that the role of PC2 in left-right patterning in all organisms may need to be reconsidered.

In addition, the mechanism by which PC2 acts in any organism to affect asymmetric events is still unclear. In mouse, PC2 is thought to act at the node to affect left-right patterning. Zebrafish *pkd2* is expressed in Kupffer's vesicle, the proposed node-equivalent in teleosts, and Bisgrove et al. report a role for *pkd2* in this structure (Bisgrove et al., 2005). A recent model proposes that activity in the mouse node provides a subtle asymmetry on the left side that manifests into robust expression of *Nodal* in the left LPM through a combination of activating signals on the left and repressive signals on the right (Nakamura et al., 2006). PC2 may be acting from within Kupffer's vesicle to initially bias the activation of *spaw* gene expression to the left side of the organism. Alternatively, PC2 might be responsible for repressing Nodal signaling on the right half of the embryo (Fig. 7). Based on *pkd2* expression data, this repression could take place at multiple sites in the embryo, including Kupffer's vesicle and the floorplate. As no midline defect is apparent in *cup* mutants, we believe that it is unlikely that PC2 in the floorplate is responsible for restricting *spaw* to the left side, but this has not been formally proven. If *pkd2* is acting at multiple levels to affect the direction of *spaw* activation and *spaw* propagation, Nakamura's model (Nakamura et al., 2006) predicts that the majority of embryos would display bilateral expression of *spaw*, which is what we observe. This model also explains how alterations in *Nodal* initiation and propagation can result in right-sided or no expression of *Nodal*, which we observe in a low percentage of *cup* mutants.

Our results also suggest that maternal *pkd2* might play a role in proper mesendoderm patterning of the visceral organs. Thus, it is possible that the effects of *pkd2* on left-right patterning could occur prior to the formation of Kupffer's vesicle. Interestingly, in *Xenopus*, there is evidence that indicates an earlier non-ciliary role for PC2 in left-right patterning prior to gastrulation (Qiu et al., 2005).

A possible role for Cup in mesendoderm patterning

We find that *pkd2* is expressed maternally in zebrafish, and has restricted expression to mesendoderm during early epiboly and gastrulation. Our work with MOs suggests that *pkd2* may play a role in the patterning of the mesendoderm. For example, at high doses of MO against *pkd2*, various mesendoderm defects are apparent, including loss of glomerular tissue in the kidney, smaller organs including the liver and gut, and thinner body axes. These defects are variable, but were seen with two different MOs against *pkd2* and are thus likely to be specific defects. The *Pkd2* knockout mouse also displays pancreatic, liver, kidney and cardiac complications at early developmental stages, further supporting a function for PC2 in mesoderm and endoderm (Wu et al., 2000).

Although low levels of MO against *pkd2* phenocopied the left-right defects seen in zygotic *cup* mutants, we believe *cup* mutants are a better system for studying the role of *pkd2* in left-right patterning. In fact, while this manuscript was in preparation, another study was published on *pkd2* using MOs in zebrafish that came to different conclusions on the role of *pkd2* in left-right patterning (Bisgrove et al., 2005). We believe that the differences in our conclusions might be due in part to the additional effects of the *pkd2* MO on the mesendoderm, which are not seen in zygotic *cup* mutants.

Similarly, zygotic *cup* embryos do not develop pronephric cysts during larval development as would be predicted for a mutation in a gene that causes polycystic kidney disease in other vertebrates. Although we could detect dilations in the pronephric region of wild-type embryos injected with a high concentration of *pkd2* augMO, histological sections revealed that the cystic tissue had an unconventional morphology as compared with other cystic mutants in the laboratory (our unpublished data). We believe the MO-specific phenotype in the kidney is due to the knockdown of maternal *pkd2* mRNA that is present in zygotic *cup* mutants, similar to what has been proposed previously (Sun et al., 2004), but because mesendoderm defects are apparent in *pkd2* morphants, the cystic kidney phenotype is questionable in its origin. Although MO knockdown of *pkd2* could be affecting redundancies in *pkd2* or alternative splice forms, we have found no evidence for the existence of these to date. We attempted to analyze protein knockdown in mutants and morphants using several antibodies against human and mouse PC2, but none of these antibodies were able to cross-react with the zebrafish protein as assessed by whole-mount in situ hybridization or western blotting. Future studies on whether maternal *pkd2* mRNA is affecting early mesendoderm patterning will be needed to fully understand the dilated kidney phenotype we observe in the morphants.

Organ laterality defects in *cup* mutants suggest multiple levels of regulation in left-right patterning

Visceral organ patterning is affected in *cup* mutants and can be categorized into three main sub-groups: normal organ positioning, situs inversus, and heterotaxia. It is intriguing that each phenotypic group constitutes about one-third of the total population of *cup* mutants, and we see similar segregation in other asymmetry mutants in our laboratory (our unpublished results). It has been proposed that in the absence of asymmetric signaling, each organ will randomly adopt a position on the left-right axis resulting in a high degree of heterotaxia (Burdine and Schier, 2000; Concha et al., 2000; Yan et al., 1999). The fact that such a large population of mutants with altered *spaw* signaling retains either wild-type or completely inverted patterning is unexpected and suggests some global left-right information is still retained when asymmetric Nodal signaling is disrupted. This idea is further supported by the finding that whereas over 30% of *cup* mutant embryos show complete situs inversus, only a small percentage of them show right-sided *spaw* expression. We have shown that the expression of downstream asymmetric genes depends on the magnitude of *spaw* expression on each side, and thus it is important to incorporate the expression patterns of multiple Nodal pathway signals in a model of how asymmetric *nodal* genes translate into the proper positioning of the organs.

cup mutants also show a loss of asymmetric gene expression in the dorsal diencephalon of the brain at 24 somites and randomized asymmetric placement of the parapineal and dorsal habenula. These data are consistent with the phenotypes of other mutants that lack Nodal signaling in the zebrafish brain (Concha et al., 2000). *cup* embryos are unique, though, in their ability to activate Nodal pathway gene expression in the LPM but not in the diencephalon of most mutants. It is intriguing to speculate that the activation of *nodal*

genes in the brain might also be dependent on the anterior propagation of *spaw* in the LPM, or upon *pkd2* activity in the diencephalon.

We thank Robert Geisler and members of the Geisler laboratory for the original bulked segregant analysis that placed *cup* onto chromosome 1; Joe Yost and Brent Bisgrove for fruitful discussions and for sharing data prior to publication; Zhoaxia Sun for providing an aliquot of the hi4166 morpholino; members of the zebrafish community for providing in situ plasmids; and Liz Gavis, Trudi Schupbach, Marc F. Schwartz, Eric Wieschaus and members of the Burdine laboratory for comments on the work and manuscript. This work was funded in part by awards to R.D.B. from the American Heart Association. R.D.B. is the 44th Mallinckrodt Scholar of the Edward Mallinckrodt Junior Foundation.

References

Ahmad, N., Long, S. and Rebagliati, M. (2004). A southpaw joins the roster: the role of the zebrafish nodal-related gene southpaw in cardiac LR asymmetry. *Trends Cardiovasc. Med.* **14**, 43-49.

Alexander, J. and Stainier, D. Y. (1999). A molecular pathway leading to endoderm formation in zebrafish. *Curr. Biol.* **9**, 1147-1157.

Amack, J. D. and Yost, H. J. (2004). The T box transcription factor no tail in ciliated cells controls zebrafish left-right asymmetry. *Curr. Biol.* **14**, 685-690.

Bisgrove, B. W., Essner, J. J. and Yost, H. J. (1999). Regulation of midline development by antagonism of lefty and nodal signaling. *Development* **126**, 3253-3262.

Bisgrove, B. W., Snarr, B. S., Emrazian, A. and Yost, H. J. (2005). Polaris and Polycystin-2 in dorsal forerunner cells and Kupffer's vesicle are required for specification of the zebrafish left-right axis. *Dev. Biol.* **287**, 274-288.

Boettger, T., Wittler, L. and Kessel, M. (1999). FGF8 functions in the specification of the right body side of the chick. *Curr. Biol.* **9**, 277-280.

Brand, M., Heisenberg, C. P., Jiang, Y. J., Beuchle, D., Lun, K., Furutani-Seiki, M., Granato, M., Haffter, P., Hammerschmidt, M., Kane, D. A. et al. (1996). Mutations in zebrafish genes affecting the formation of the boundary between midbrain and hindbrain. *Development* **123**, 179-190.

Burdine, R. D. and Schier, A. F. (2000). Conserved and divergent mechanisms in left-right axis formation. *Genes Dev.* **14**, 763-776.

Chen, J. N., van Eeden, F. J., Warren, K. S., Chin, A., Nusslein-Volhard, C., Haffter, P. and Fishman, M. C. (1997). Left-right pattern of cardiac BMP4 may drive asymmetry of the heart in zebrafish. *Development* **124**, 4373-4382.

Cleaver, O. B., Patterson, K. D. and Krieg, P. A. (1996). Overexpression of the tinman-related genes XNkx-2.5 and XNkx-2.3 in Xenopus embryos results in myocardial hyperplasia. *Development* **122**, 3549-3556.

Concha, M. L., Burdine, R. D., Russell, C., Schier, A. F. and Wilson, S. W. (2000). A nodal signaling pathway regulates the laterality of neuroanatomical asymmetries in the zebrafish forebrain. *Neuron* **28**, 399-409.

Delmas, P., Padilla, F., Osorio, N., Coste, B., Raoux, M. and Crest, M. (2004). Polycystins, calcium signaling, and human diseases. *Biochem. Biophys. Res. Commun.* **322**, 1374-1383.

Essner, J. J., Branford, W. W., Zhang, J. and Yost, H. J. (2000). Mesendoderm and left-right brain, heart and gut development are differentially regulated by pitx2 isoforms. *Development* **127**, 1081-1093.

Essner, J. J., Vogan, K. J., Wagner, M. K., Tabin, C. J., Yost, H. J. and Brueckner, M. (2002). Conserved function for embryonic nodal cilia. *Nature* **418**, 37-38.

Essner, J. J., Amack, J. D., Nyholm, M. K., Harris, E. B. and Yost, H. J. (2005). Kupffer's vesicle is a ciliated organ of asymmetry in the zebrafish embryo that initiates left-right development of the brain, heart and gut. *Development* **132**, 1247-1260.

Fischer, A., Viebahn, C. and Blum, M. (2002). FGF8 acts as a right determinant during establishment of the left-right axis in the rabbit. *Curr. Biol.* **12**, 1807-1816.

Gamse, J. T., Shen, Y. C., Thisse, C., Thisse, B., Raymond, P. A., Halpern, M. E. and Liang, J. O. (2002). Otx5 regulates genes that show circadian expression in the zebrafish pineal complex. *Nat. Genet.* **30**, 117-121.

Gamse, J. T., Thisse, C., Thisse, B. and Halpern, M. E. (2003). The parapineal mediates left-right asymmetry in the zebrafish diencephalon. *Development* **130**, 1059-1068.

Gonzalez-Perrett, S., Kim, K., Ibarra, C., Damiano, A. E., Zotta, E., Batelli, M., Harris, P. C., Reisin, I. L., Arnaout, M. A. and Cantiello, H. F. (2001). Polycystin-2, the protein mutated in autosomal dominant polycystic kidney disease (ADPKD), is a Ca2+-permeable nonselective cation channel. *Proc. Natl. Acad. Sci. USA* **98**, 1182-1187.

Gritsman, K., Zhang, J., Cheng, S., Heckscher, E., Talbot, W. S. and Schier, A. F. (1999). The EGF-CFC protein one-eyed pinhead is essential for nodal signaling. *Cell* **97**, 121-132.

Haffter, P., Granato, M., Brand, M., Mullins, M. C., Hammerschmidt, M., Kane, D. A., Odenthal, J., van Eeden, F. J., Jiang, Y. J., Heisenberg, C. P. et al. (1996). The identification of genes with unique and essential functions in the development of the zebrafish, Danio rerio. *Development* **123**, 1-36.

Hanaoka, K., Qian, F., Boletta, A., Bhunia, A. K., Piontek, K., Tsiokas, L., Sukhatme, V. P., Guggino, W. B. and Germino, G. G. (2000). Co-assembly of polycystin-1 and -2 produces unique cation-permeable currents. *Nature* **408**, 990-994.

Hashimoto, H., Rebagliati, M., Ahmad, N., Muraoka, O., Kurokawa, T., Hibi, M. and Suzuki, T. (2004). The Cerberus/Dan-family protein Charon is a negative regulator of Nodal signaling during left-right patterning in zebrafish. *Development* **131**, 1741-1753.

Hayashi, T., Mochizuki, T., Reynolds, D. M., Wu, G., Cai, Y. and Somlo, S. (1997). Characterization of the exon structure of the polycystic kidney disease 2 gene (PKD2). *Genomics* **44**, 131-136.

Kramer-Zucker, A. G., Olale, F., Haycraft, C. J., Yoder, B. K., Schier, A. F. and Drummond, I. A. (2005). Cilia-driven fluid flow in the zebrafish pronephros, brain and Kupffer's vesicle is required for normal organogenesis. *Development* **132**, 1907-1921.

Krauss, S., Concordet, J. P. and Ingham, P. W. (1993). A functionally conserved homolog of the Drosophila segment polarity gene hh is expressed in tissues with polarizing activity in zebrafish embryos. *Cell* **75**, 1431-1444.

Liao, E. C. and Zon, L. I. (1999). Simple sequence-length polymorphism analysis. *Methods Cell Biol.* **60**, 181-183.

Liu, S., Lu, W., Obara, T., Kuida, S., Lehoczky, J., Dewar, K., Drummond, I. A. and Beier, D. R. (2002). A defect in a novel Nek-family kinase causes cystic kidney disease in the mouse and in zebrafish. *Development* **129**, 5839-5846.

McGrath, J. and Brueckner, M. (2003). Cilia are at the heart of vertebrate left-right asymmetry. *Curr. Opin. Genet. Dev.* **13**, 385-392.

McGrath, J., Somlo, S., Makova, S., Tian, X. and Brueckner, M. (2003). Two populations of node monocilia initiate left-right asymmetry in the mouse. *Cell* **114**, 61-73.

Mercola, M. and Levin, M. (2001). Left-right asymmetry determination in vertebrates. *Annu. Rev. Cell Dev. Biol.* **17**, 779-805.

Meyers, E. N. and Martin, G. R. (1999). Differences in left-right axis pathways in mouse and chick: functions of FGF8 and SHH. *Science* **285**, 403-406.

Milewski, W. M., Duguay, S. J., Chan, S. J. and Steiner, D. F. (1998). Conservation of PDX-1 structure, function, and expression in zebrafish. *Endocrinology* **139**, 1440-1449.

Nakamura, T., Mine, N., Nakaguchi, E., Mochizuki, A., Yamamoto, M., Yashiro, K., Meno, C. and Hamada, H. (2006). Generation of robust left-right asymmetry in the mouse embryo requires a self-enhancement and lateral-inhibition system. *Dev. Cell* **11**, 495-504.

Nauli, S. M., Alenghat, F. J., Luo, Y., Williams, E., Vassilev, P., Li, X., Elia, A. E., Lu, W., Brown, E. M., Quinn, S. J. et al. (2003). Polycystins 1 and 2 mediate mechanosensation in the primary cilium of kidney cells. *Nat. Genet.* **33**, 129-137.

Odenthal, J. and Nusslein-Volhard, C. (1998). fork head domain genes in zebrafish. *Dev. Genes Evol.* **208**, 245-258.

Ohara, O., Dorit, R. L. and Gilbert, W. (1989). One-sided polymerase chain reaction: the amplification of cDNA. *Proc. Natl. Acad. Sci. USA* **86**, 5673-5677.

Okada, Y., Takeda, S., Tanaka, Y., Belmonte, J. C. and Hirokawa, N. (2005). Mechanism of nodal flow: a conserved symmetry breaking event in left-right axis determination. *Cell* **121**, 633-644.

Otto, E. A., Schermer, B., Obara, T., O'Toole, J. F., Hiller, K. S., Mueller, A. M., Ruf, R. G., Hoefele, J., Beekmann, F., Landau, D. et al. (2003). Mutations in INVS encoding inversin cause nephronophthisis type 2, linking renal cystic disease to the function of primary cilia and left-right axis determination. *Nat. Genet.* **34**, 413-420.

Pennekamp, P., Karcher, C., Fischer, A., Schweickert, A., Skryabin, B., Horst, J., Blum, M. and Dworniczak, B. (2002). The ion channel polycystin-2 is required for left-right axis determination in mice. *Curr. Biol.* **12**, 938-943.

Qiu, D., Cheng, S. M., Wozniak, L., McSweeney, M., Perrone, E. and Levin, M. (2005). Localization and loss-of-function implicates ciliary proteins in early, cytoplasmic roles in left-right asymmetry. *Dev. Dyn.* **234**, 176-189.

Ramsdell, A. F. (2005). Left-right asymmetry and congenital cardiac defects: getting to the heart of the matter in vertebrate left-right axis determination. *Dev. Biol.* **288**, 1-20.

Raya, A., Kawakami, Y., Rodriguez-Esteban, C., Ibanes, M., Rasskin-Gutman, D., Rodriguez-Leon, J., Buscher, D., Feijo, J. A. and Izpisua Belmonte, J. C. (2004). Notch activity acts as a sensor for extracellular calcium during vertebrate left-right determination. *Nature* **427**, 121-128.

Roessler, E. and Muenke, M. (2001). Midline and laterality defects: left and right meet in the middle. *BioEssays* **23**, 888-900.

Sarmah, B., Latimer, A. J., Appel, B. and Wente, S. R. (2005). Inositol polyphosphates regulate zebrafish left-right asymmetry. *Dev. Cell* **9**, 133-145.

Struhl, G. (1981). Anterior and posterior compartments in the proboscis of Drosophila. *Dev. Biol.* **84**, 372-385.

Sun, Z. and Hopkins, N. (2001). vhnf1, the MODY5 and familial GCKD-associated gene, regulates regional specification of the zebrafish gut, pronephros, and hindbrain. *Genes Dev.* **15**, 3217-3229.

Sun, Z., Amsterdam, A., Pazour, G. J., Cole, D. G., Miller, M. S. and Hopkins, N. (2004). A genetic screen in zebrafish identifies cilia genes as a principal cause of cystic kidney. *Development* **131**, 4085-4093.
Tabin, C. J. and Vogan, K. J. (2003). A two-cilia model for vertebrate left-right axis specification. *Genes Dev.* **17**, 1-6.
Talbot, W. S. and Schier, A. F. (1999). Positional cloning of mutated zebrafish genes. *Methods Cell Biol.* **60**, 259-286.
Thisse, C. and Thisse, B. (1999). Antivin, a novel and divergent member of the TGFbeta superfamily, negatively regulates mesoderm induction. *Development* **126**, 229-240.
Vassilev, P. M., Guo, L., Chen, X. Z., Segal, Y., Peng, J. B., Basora, N., Babakhanlou, H., Cruger, G., Kanazirska, M., Ye, C. et al. (2001). Polycystin-2 is a novel cation channel implicated in defective intracellular Ca(2+) homeostasis in polycystic kidney disease. *Biochem. Biophys. Res. Commun.* **282**, 341-350.
Webb, S. E. and Miller, A. L. (2000). Calcium signalling during zebrafish embryonic development. *BioEssays* **22**, 113-123.
Wu, G., Mochizuki, T., Le, T. C., Cai, Y., Hayashi, T., Reynolds, D. M. and Somlo, S. (1997). Molecular cloning, cDNA sequence analysis, and chromosomal localization of mouse Pkd2. *Genomics* **45**, 220-223.
Wu, G., Markowitz, G. S., Li, L., D'Agati, V. D., Factor, S. M., Geng, L., Tibara, S., Tuchman, J., Cai, Y., Park, J. H. et al. (2000). Cardiac defects and renal failure in mice with targeted mutations in Pkd2. *Nat. Genet.* **24**, 75-78.
Yan, Y. T., Gritsman, K., Ding, J., Burdine, R. D., Corrales, J. D., Price, S. M., Talbot, W. S., Schier, A. F. and Shen, M. M. (1999). Conserved requirement for EGF-CFC genes in vertebrate left-right axis formation. *Genes Dev.* **13**, 2527-2537.
Yelon, D., Horne, S. A. and Stainier, D. Y. (1999). Restricted expression of cardiac myosin genes reveals regulated aspects of heart tube assembly in zebrafish. *Dev. Biol.* **214**, 23-37.